IJARSCT
ISSN (Online) 2581-9429
International Journal of Advanced Research in Science, Communication and Technology (IJARSCT)
International Open-Access, Double-Blind, Peer-Reviewed, Refereed, Multidisciplinary Online Journal
Impact Factor: 7.53
Volume 4, Issue 4, March 2024

CZTS Thin Film Solar Cell by using Electrochemical Deposition method

Prof. Gulab P Kumkar[1] and Prof. Chaudhari B. S.[2]
Professor, Department of General Science & Humanities[1]
Professor, Department of Information Technology[2]
Navsahyadri Group of Institutions, Polytechnic-Pune, Maharashtra, India

Abstract: *World has been facing energy crises due to increase in the energy demand and depletion in the reserves of conventional sources like fossil fuels. Hence the development and harnessing non-conventional sources is a need. Solar energy is the largest source of energy which if harnessed can provide 1000 times the current energy demand. Converting this energy into electricity through solar cell is one of the best ways. Silicon solar cells have been traditionally used to harness solar energy. Due to high cost and depleting reserves of Si; CIGS and CdTe solar cells came in picture which have less efficiency but at low cost. But these cells contain elements like Cd which is toxic and Te, In, Ga are costly and scarce. CZTS thin films have been deposited on conducting glass plate / glass substrates using low-cost electrode position method. In different deposition techniques for CZTS absorber layer electro deposition is an effective and low-cost alternative deposition method. CZTS solar cell can prove a substitute for those solar cell as they contain novel and earth abundant material which are easily at low cost. The synthesis of CZTS thin film using electroplating method was carried out by depositing Sn, Cu, and Zn one after the other on a single substrate. The aim of this study is to fabricate Cu_2ZnSnS_4 (CZTS) thin film by electrodepositing the metal precursor. Important electroplating variables of the electro deposition are current distribution, pH, temperature, agitation and solution composition. The process is in two steps 1) comprised the electroplating of metallic precursors. As all precursors were first fabricated on stainless steel (SS) for optimization of process then it was synthesized on FTO coated glass. 2) Second process step was sulphuration of precursors. The FE-SEM and EDS gives the concentration then XRD shows the particle size. The XRD patterns of the precursor showed the preferred orientation of the phases.*

Keywords: Diffusion limited aggregation (DLA), kesterite structure of CZTS, Sulphurization, SEM

I. INTRODUCTION

In the EIA, International energy outlook 2013 world energy consumption increases from 524 quadrillion Btu in 2010 to 630 quadrillion Btu in 2020 and 820 quadrillion Btu in 2040, a 30-year increase of 56 percent. More than 85 percent of the increase in global energy demand from 2010 to 2040 occurs among the developing nations outside the organization for Economic Cooperation and Development (OECD), driven by strong economic growth and expanding populations.

In the non-OECD nations, hydroelectric power is the predominant source of renewable energy growth, accounting for 63 percent of the total increment in non-OECD renewable energy use over the projection. Strong increases in hydroelectric generation, primarily from mid-to large scale power plants, are expected in non-OECD Asia (especially, China and India), which in combination account for 80 percent of the total increase in non-OECD hydroelectric generation from 2010-2040. Growth rates for wind powered electricity generation also are relatively high in non-OECD countries. China has one of the fastest growing non-OECD regional markets for wind power, with projected total generation from wind power plants increasing from 45 billion kilowatt-hours in 2010 to 637 billion kilowatt-hours in 2040, at an average rate 9.3 percent per year. In china, where wind generation accounted for 6 percent of total renewable generation in 2010, its share grows to 26 percent in 2040.

DOI: 10.48175/568

IJARSCT
ISSN (Online) 2581-9429
International Journal of Advanced Research in Science, Communication and Technology (IJARSCT)
International Open-Access, Double-Blind, Peer-Reviewed, Refereed, Multidisciplinary Online Journal
Impact Factor: 7.53
Volume 4, Issue 4, March 2024

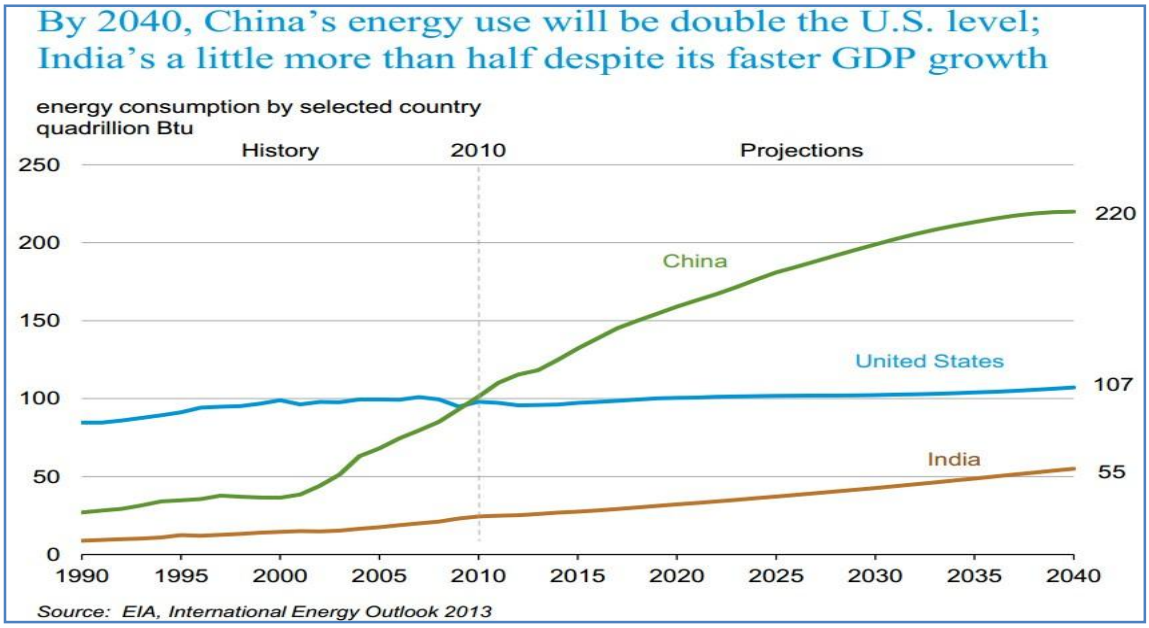

Figure: Energy consumption in US, China and India, 1990-1940

II. LITERATURE SURVEY

World net electricity generation increases by 93 percent in the IEO2013 Reference case, from 20.2 trillion kilowatt-hours in 2010 to 39.0 trillion kilowatt-hours in 2040. In general, the growth of electricity demand in the OECD countries, where electricity markets are well established and consumption patterns are mature, is slower than in the non-OECD countries, where at present many people do not have access to electricity. Total net electricity generation in non-OECD countries increases by an average of 3.1 percent per year in the Reference case, led by non-OECD Asia (including China and India), where annual increases average 3.6 percent from 2010 to 2040. In contrast, total net generation in the OECD nations grows by an average of 1.1 percent per year from 2010 to 2040.

Renewable energy and nuclear power are the world's fastest-growing energy sources, each increasing by 2.5 percent per year. However, fossil fuels continue to supply almost 80 percent of world energy use through 2040. Natural gas is the fastest-growing fossil fuel in the outlook. Global natural gas consumption increases by 1.7 percent per year. Increasing supplies of tight gas, shale gas, and coal bed methane support growth in projected worldwide natural gas use. Coal use grows faster than petroleum and other liquid fuel use until after 2030, mostly because of increases in China's consumption of coal and tepid growth in liquids demand attributed to slow growth in the OECD regions and high sustained oil prices. The industrial sector continues to account for the largest share of delivered energy consumption; the world industrial sector still consumes over half of global delivered energy in 2040. Given current policies and regulations limiting fossil fuel use, worldwide energy-related carbon dioxide emissions rise from about 31 billion metric tons in 2010 to 36 billion metric tons in 2020 and then to 45 billion metric tons in 2040, a 46-percent increase.

China and India are each pursuing an aggressive solar PV growth strategy, creating a very important industry and setting up ambitious mid-term targets for the domestic market in the multi-GW scale. Brazil is a leading country in the use of PV for rural electrification.

III. OBJECTIVE

The photovoltaic (PV) power has a particularly promising future. Global PV capacity has been increasing at an average annual growth rate of more than 40% since 2000 and it has significant potential for long-term growth over the next decades. This road maps envisions that by 2050, PV will provide 11% of global electricity production (4500TWh per year), corresponding to 3000 GW of cumulative installed PV capacity. In addition to greenhouse gas emission reductions, this level of PV will deliver substantial benefits in terms of the security of energy supply and socio-

IJARSCT
ISSN (Online) 2581-9429
International Journal of Advanced Research in Science, Communication and Technology (IJARSCT)
International Open-Access, Double-Blind, Peer-Reviewed, Refereed, Multidisciplinary Online Journal
Impact Factor: 7.53
Volume 4, Issue 4, March 2024

economic development. Solar cells utilize the mechanism of photoelectric effect and converting sunlight directly into electricity without any intermediate steps. Solar cells are easy to install and use and their operational lifetimes are long with minimum maintenance. To enhance the current conversion efficiency and to develop low-cost cells, widespread research investigations are being conducted. The main component of a solar cell is the light absorber material.

CopperzinctinsulfideCu_2ZnSnS_4 (CZTS) is a quaternary semiconducting compound which has received increasing interest since the late 2000s for applications in solar cells. The class of related materials includes other I_2-II-IV-VI_4 such as copper zinc tin selenide (CZTSe) and the sulfur-selenium alloy CZTSSe. CZTS offers favorable optical and electronic properties similar to CIGS (copper indium gallium selenide) making it well suited for use as a thin-film solar cell absorber layer, but unlike CIGS (or other thin films such as CdTe), CZTS is composed of only abundant and non-toxic elements. Concerns with the price and availability of indium in CIGS and tellurium inCdTe, as well as toxicity of cadmiumhave been a large motivator to search for alternative thinfilmsolarcell materials. Recent material improvements for CZTS have increased efficiency to 12.0% in laboratory cells, but more work is needed for their commercialization

IV. TOOLS AND TECHNOLOGY

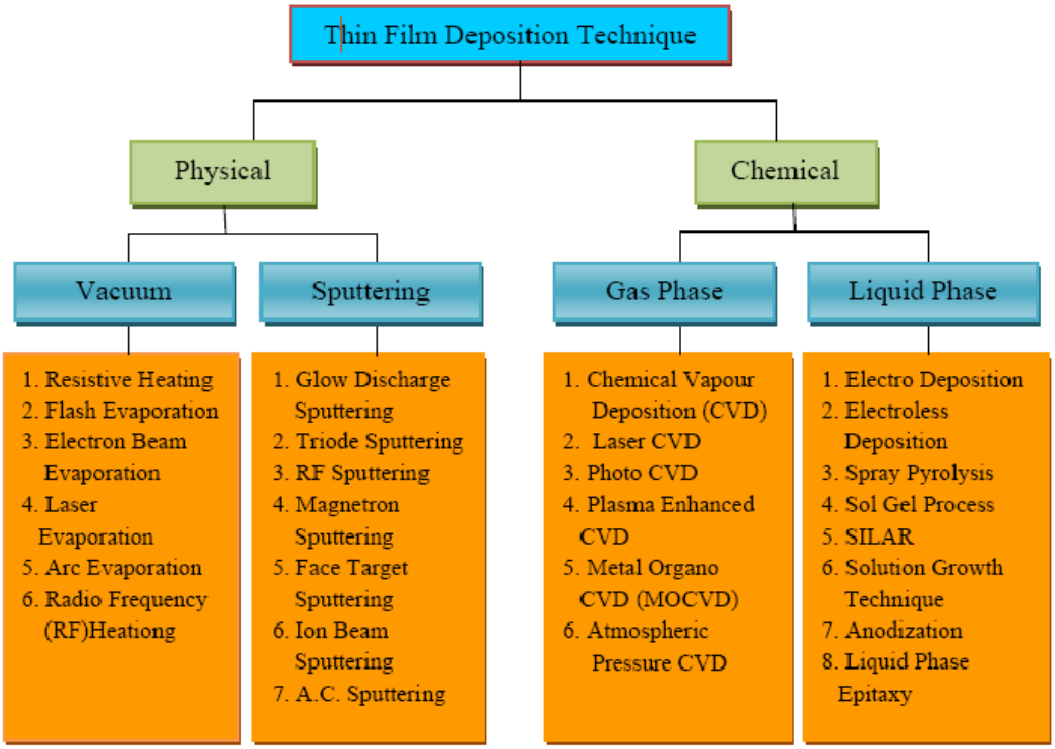

Mechanism of Electrodeposition:

Electrodeposition is process of depositing metal atoms on a conducting substrateby passing direct current through solution containing the metal(s) ions to be deposited.The schematic diagram explaining the electrodeposition is shown in figure 2.1.The typical electrodeposition set up consists of following,

1. Electrolyte
2. Cathode and anode
3. Source of electricity.

When direct current is passed through cathode and anode, immersed in electrolytecontaining the metal(s) ions, the metal ions get attracted towards the cathode,neutralized electrically by receiving electrons and get deposited on cathode. Thedeposition is controlled by monitoring the amount and the rate of charge passingthrough the electrolyte. Thus the electrical energy is used to cause chemical change.

IJARSCT
ISSN (Online) 2581-9429
International Journal of Advanced Research in Science, Communication and Technology (IJARSCT)
International Open-Access, Double-Blind, Peer-Reviewed, Refereed, Multidisciplinary Online Journal
Impact Factor: 7.53
Volume 4, Issue 4, March 2024

Analysis Techniques

X-ray diffraction method (XRD)

During the experiments we used several different measuring techniques to retrievethe information needed from the various samples. Properties of interestwere energy band gap, film thickness, stoichiometry and surface morphology.The techniques used to determine these characteristics will be explained here.X-ray diffractionX-ray diffraction (XRD) is a technique based on Bragg's law, a geometric lawwhich allows crystallographic properties of the film to be retrieved. Bragg'slaw can be deduced from the geometry of below figure, and is given in thefollowing formula:

$n\lambda = 2d\sin(\theta)$

Where n is an integer, λ is the wavelength of the incoming X-rays, d is thedistance between crystal planes, and θ -the angle of incidence of the X-rays.

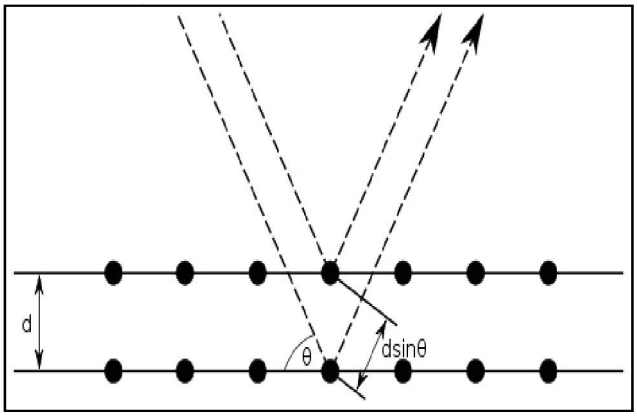

Figure: Geometry of Bragg diffraction.

Scanning electron microscopy

Scanning electron microscopy (SEM) is a method to determine surface morphology of a sample. Additionally, some SEM setups have an X-ray detector to perform EDX measurements. A standard SEM setup is shown in figure.

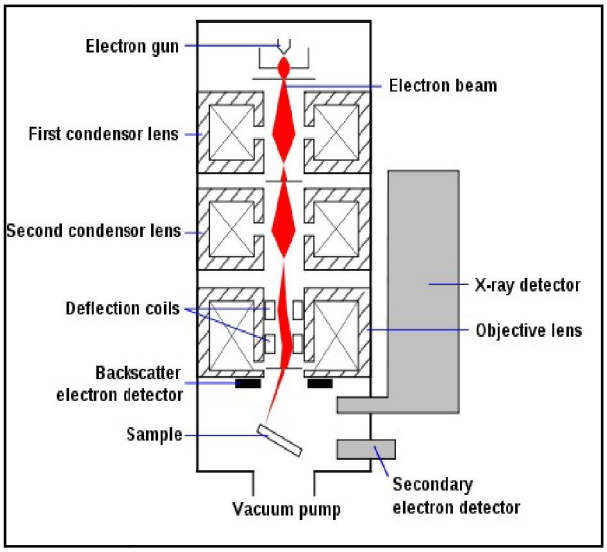

Figure: Typical SEM setup.

Raman Spectral Study

Raman spectroscopy is different from the rotational and vibrational spectroscopyconsidered above in that it is concern with the scattering of radiation by the simple,rather than an absorption process. It is named after the Indian physicists

IJARSCT
ISSN (Online) 2581-9429
International Journal of Advanced Research in Science, Communication and Technology (IJARSCT)
International Open-Access, Double-Blind, Peer-Reviewed, Refereed, Multidisciplinary Online Journal
Impact Factor: 7.53
Volume 4, Issue 4, March 2024

who firstobserve it in 1928, C. V. Raman. Both rotational and vibrational spectroscopes arepossible. The energy of the exciting radiation will determine which type of the transitionoccurs-rotational transitions are lower in energy than vibrational transitions.In addition to this, rotational transitions are around three orders of magnitudeslower than vibrational transitions. Therefore, collisions with other molecule may occurin the time in which the transition is occurring. A collision is likely to change therotational state of the molecule, and so the definition of the spectrum obtained willdestroyed. Rotational spectroscopy is therefore carried out on gases at low pressure toensure that the time between the collisions is greater than the time for transition.

The basic set up of Raman spectrometer is shown below.

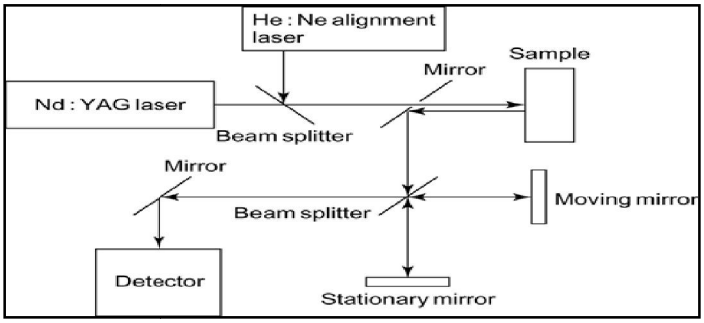

Figure: Basic set up of Raman Spectrometer**.**

V. ACTIVITY DIAGRAM

The synthesis of CZTS thin films using electroplating method was carried out by depositing Cu, Zn, and Sn on substrate respectively. For this purpose, the chemicals used were $CuSO_4$, $ZnCl_2$,and SnCl2. These chemicals were used as sources of Cu, Zn, Sn respectively. At first the concentration of solutions was optimized on trial basis. The films were electrodeposited in a vertical cell in which the electrodes (both working and counter) were suspended vertically from the top of cell. Precursor films were prepared by employing a two-electrode cell in which the counter electrode was graphite and the working electrode (substrate) was ITO glass and SS (Stainless steel). Theelectrodeposition processes were performed in a RADIAL DC regulated Power supply. During electrochemical cell contains a counter electrode as graphite electrode and Working electrode as a SS (stainless steel) / FTO electrode, with deposition area of 2×4 cm^2 was used as working electrode. The CZTS thin films were prepared from aqueous electrolytic bath containing copper sulfate Pentahydrate ($CuSO_4 \cdot 5H_2O$), zinc chloride ($ZnCl_2$), stannous chloride ($Sncl_2.2H_20$)using a layer-by-layer electrodeposition method at room temperature for 60 min. Ammonia (NH3) as complexing agent and Hydrochloric acid (HCL) as pH control solution were used. The pH concentration was maintained to 5. The CZTS thin films were deposited by potentiostatic electrodeposition at an applied potential of 2.05 V

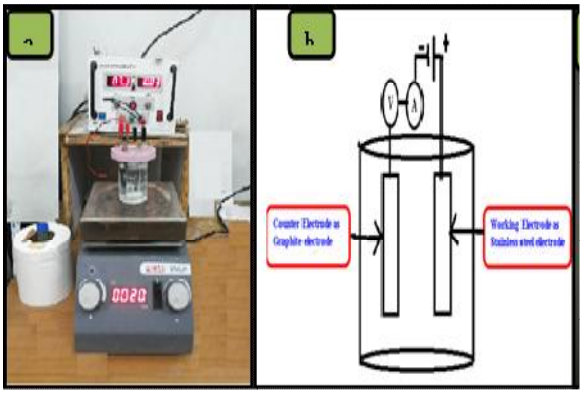

Figure: (a) Schematic diagram of the electro deposition of CZT absorber layers from successive electroplating method. (b) Counter electrode and working electrode are connected by DC regulator Power supply. (c) Images of stainless steel (SS) and graphite

IJARSCT
ISSN (Online) 2581-9429
International Journal of Advanced Research in Science, Communication and Technology (IJARSCT)
International Open-Access, Double-Blind, Peer-Reviewed, Refereed, Multidisciplinary Online Journal
Impact Factor: 7.53
Volume 4, Issue 4, March 2024

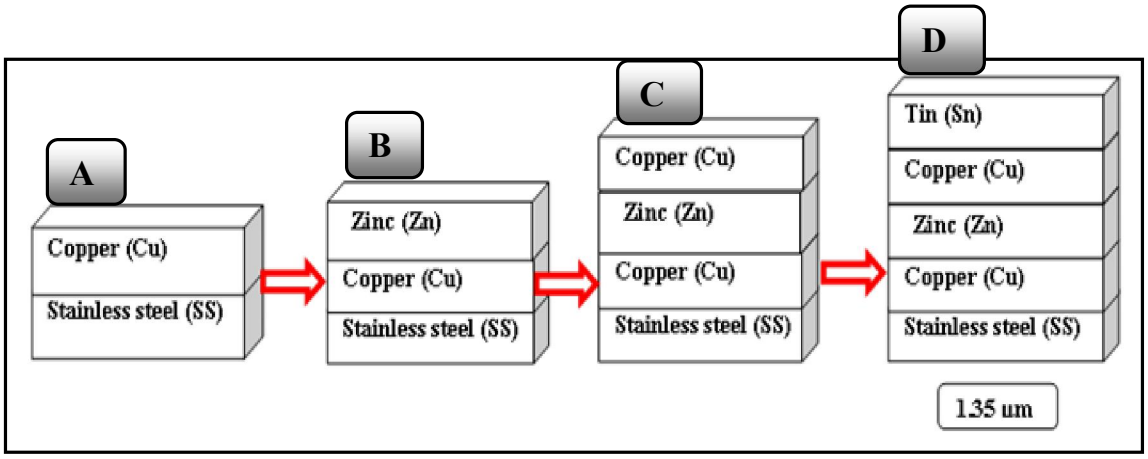

Figure: schematic of CZTS film layer by layer.

Sulphurization

Sulphurization is the process of annealing in the sulphur atmosphere. In this process the substrate is heated in presence of sulphur in furnace. For this, 1 gm solid sulphur is taken in crucible and the substrate is hung in such a way over it. Such that the sulphur vapors get deposited on the previously deposited layers. The sulphurization is done at different temperatures.

The sulphurization gives the final layer of CZTS thin film. It not only adds up sulphur, but it forms a homogeneous film of the layers due to annealing at such high temperature. This film was then characterized. After the confirmation from the characterization results, the substrate was changed to molybdenum (Mo), so that the thin film so formed can be used for solar cell construction.

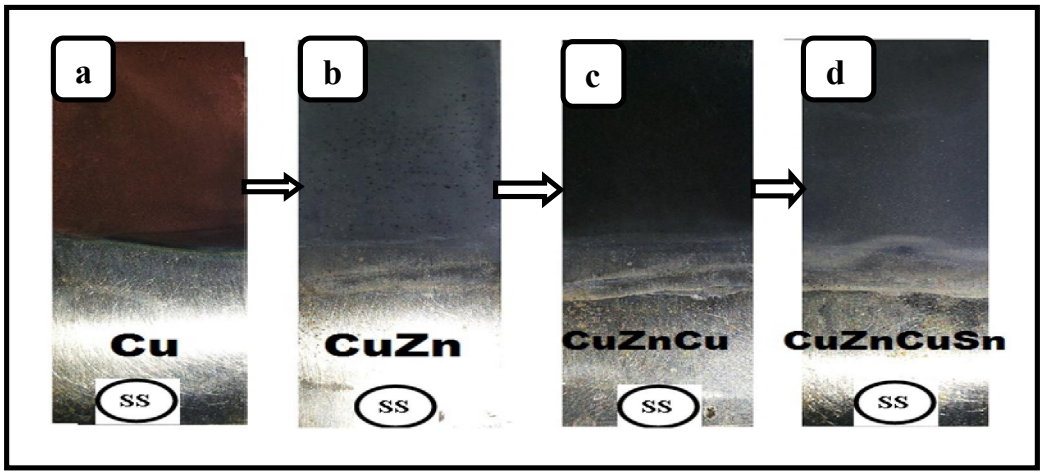

Figure: effect of electro deposition on stainless steel (SS)

IJARSCT
ISSN (Online) 2581-9429
International Journal of Advanced Research in Science, Communication and Technology (IJARSCT)
International Open-Access, Double-Blind, Peer-Reviewed, Refereed, Multidisciplinary Online Journal
Impact Factor: 7.53
Volume 4, Issue 4, March 2024

VI. RESULT AND CONCLUSION

As-deposited CZT thin films

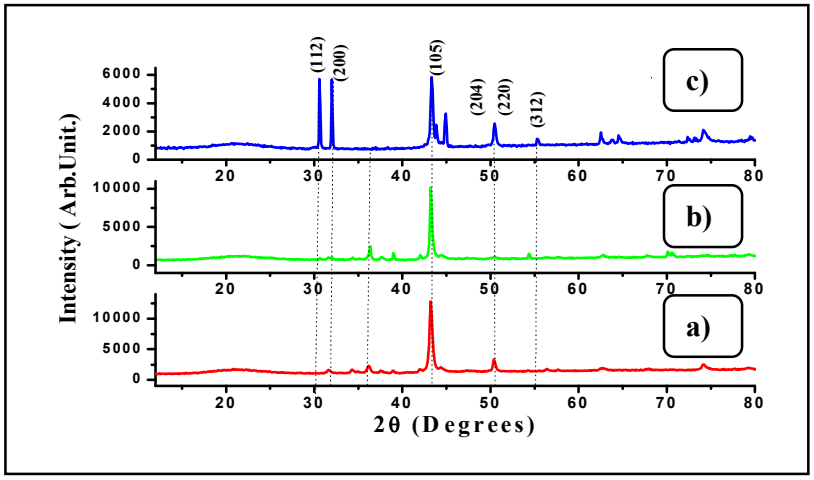

Figure: XRD pattern of as-deposited CZT thin films on stainless steel (SS) substrate

Above figure shows that XRD Spectra of CZT thin films deposited on stainless steel substrate, which indicates that formation of chalcopyrite structure on SS. (112), (200), (105), (204), (220) and (312) miller indices of peaks represents the crystalline phase of CZT (alloy) material, Initiating peaks of (112) and (200) found in a), b) and c). SS peaks also observed in XRD spectra of CZT materials, the Miller indices of plane consisting with standard JCPDS data of Chalcopyrite structure.

Annealed CZT thin films converted into CZTS

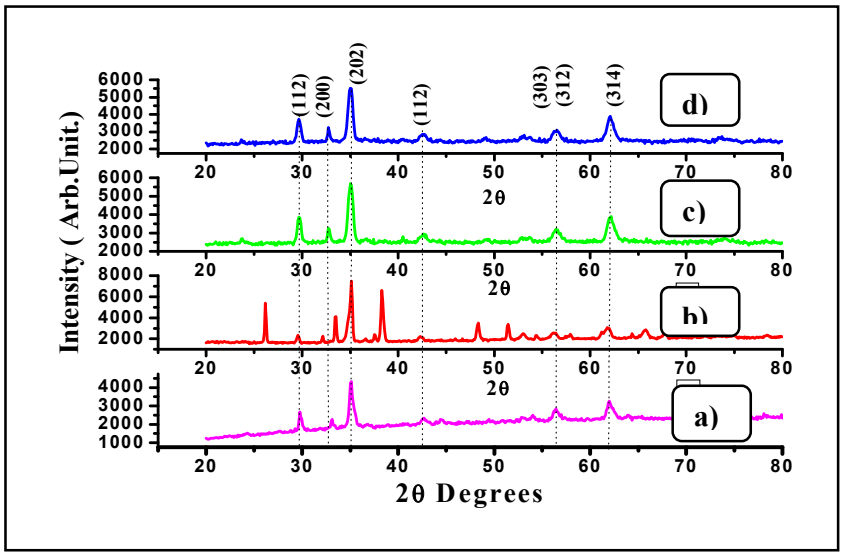

Figure: XRD pattern of Annealed CZT thin film converted in to CZTS thin films at **800^{0}C**

CZT thin films alloy is annealed at 800^{0}C in presence of sulphur atmosphere, all metallic layers are miscible at high temperature. The decomposition of CZT alloys at 200^0 C temperatures. The Chalcopyrite phases of CZT alloy are transfer into tetragonal phase, which is appeared in XRD pattern. XRD graph confirmed tetragonal structure with lattice parameter, a=b=5.427 **Å**, c=10.84 **Å,** which is consistent with standard JCPDS, Data file 260575 of inter planer distance, 2θ degrees, and miller indices plane CZTS is (112), (220), (303) and (312).

IJARSCT
ISSN (Online) 2581-9429
International Journal of Advanced Research in Science, Communication and Technology (IJARSCT)
International Open-Access, Double-Blind, Peer-Reviewed, Refereed, Multidisciplinary Online Journal
Impact Factor: 7.53
Volume 4, Issue 4, March 2024

(hkl) Plane	2θ	θ	Sin(θ)	2sin(θ)	Standard (d) Å	Observed (d) Å
110	23.79	11.89	0.02060	0.4120	3.84	3.73
103	29.7	14.85	0.2562	0.5125	3.008	3.00
200	32.80	16.80	0.2890	0.5780	2.71	2.66
202	35.12	17.56	0.3017	0.6034	2.42	2.55
105	42.49	21.24	0.3662	0.7245	2.01	2.12
220	49.03	24.51	0.4118	0.8297	1.91	1.85
303/312	56.62	28.31	0.4742	0.9484	1.638	1.62
314	62.16	31.08	0.5162	1.0324	1.45	1.49

Table: 1 XRD data calculation

Surface morphology

As-deposited CZT thin films

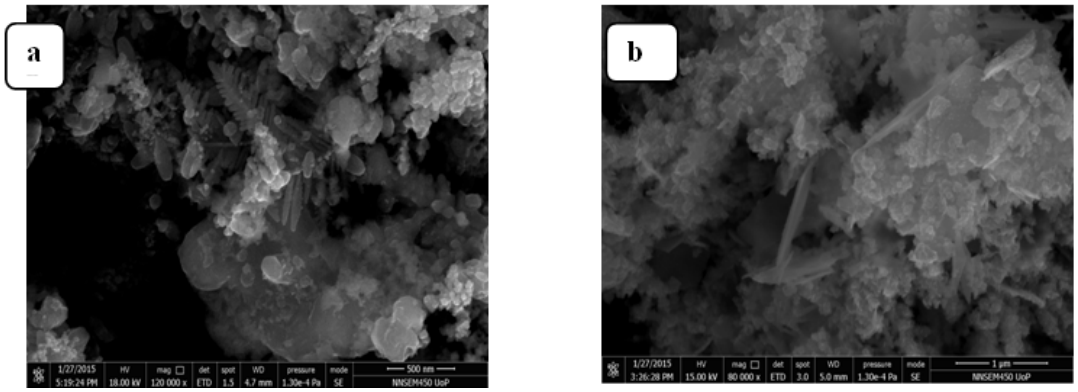

Figure: Surface electron micrograph of as-deposited CZT alloy thin films studied by FE- SEM

Fig. a) Shows that the surface micrograph of CZT alloy on SS materials, which is appear as a leaf of fern and irregular aggregate of granular grain on the surface of SS materials. Diffusion limited aggregation (DLA) was found in fern leaves. Fig.b) represents a flake like structure as well as irregular aggregate of granular grain on the surface of SS materials respectively at room temperature.

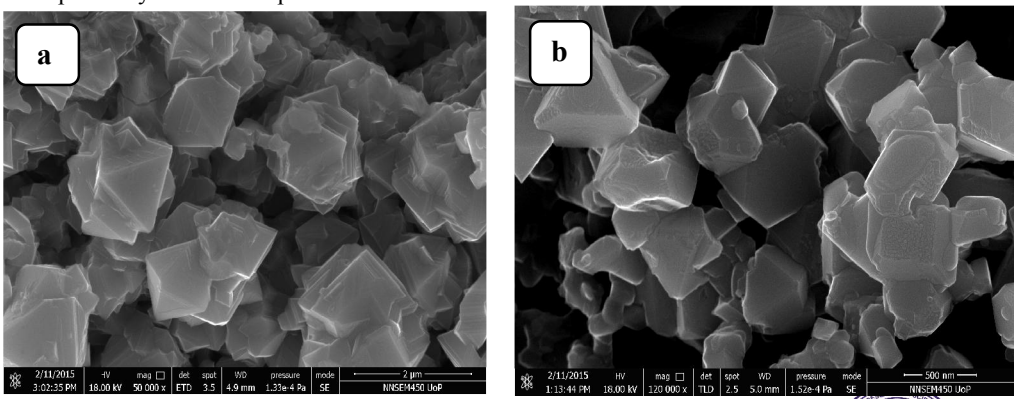

Figure: Surface electron micrograph of annealed CZT in sulphur at 300^{0}C

IJARSCT
ISSN (Online) 2581-9429
International Journal of Advanced Research in Science, Communication and Technology (IJARSCT)
International Open-Access, Double-Blind, Peer-Reviewed, Refereed, Multidisciplinary Online Journal
Impact Factor: 7.53
Volume 4, Issue 4, March 2024

Figure: a) and b) shows that a surface electron micrograph of well-defined grain size is about 2µm and 500 nm scale of CZTS material respectively. The Sharp edges tetragonal diamond like shape on SS materials at 2µm scale of SEM.

Raman shift

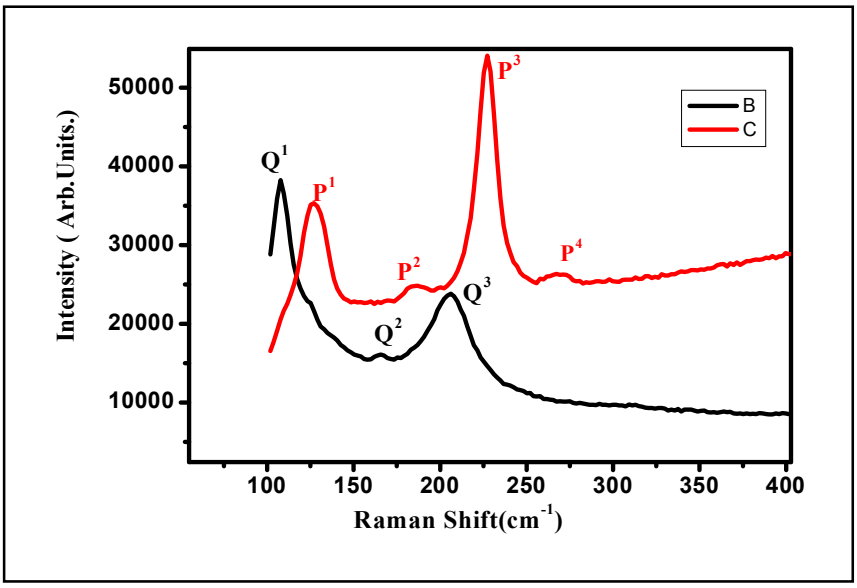

Figure: Raman spectra of as deposited CZT materials.

In above figureRaman spectra of as -deposited CZT materials has intermetallic phases of CuZn, CuZnSn, CuSn, Cu, Zn and Sn respectively.

Phase	Raman Scattering peak (cm^{-1})	
	Sample (B)	Sample (c)
Intermetallic Phase	100 P^1	125 Q1
Intermetallic Phase	160 P^2	160 Q2
Intermetallic Phase	210 P^3	210 Q3
Intermetallic phase	275 P^4	----

Table: summary of the Raman peaks location of CZT phases.

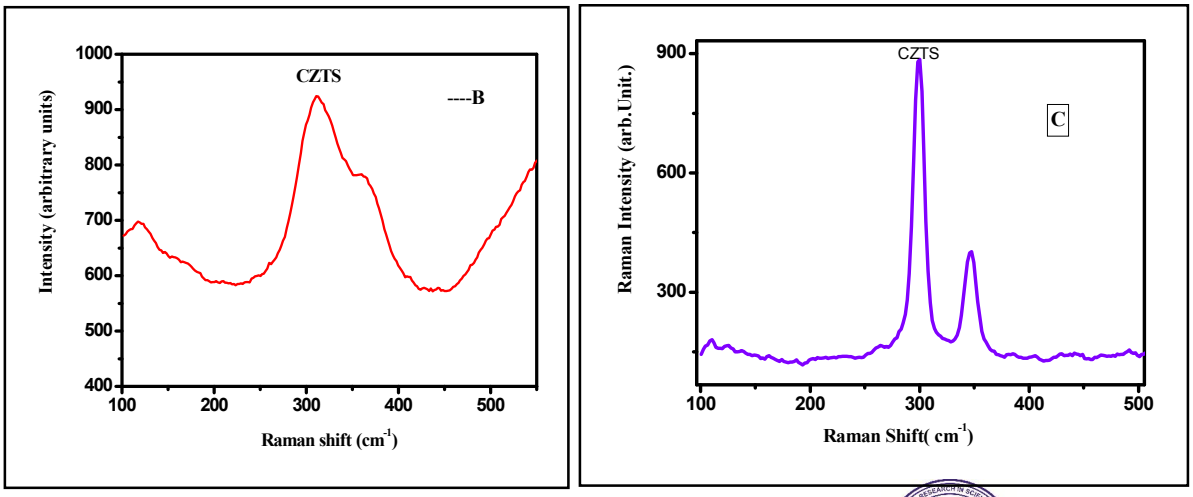

Figure: Raman spectra of annealed sample CZTS thin films

IJARSCT
ISSN (Online) 2581-9429
International Journal of Advanced Research in Science, Communication and Technology (IJARSCT)
International Open-Access, Double-Blind, Peer-Reviewed, Refereed, Multidisciplinary Online Journal
Impact Factor: 7.53
Volume 4, Issue 4, March 2024

Phase	Raman Scattering peak (cm^{-1})		References
	Sample(B)	Sample (c)	
CZTS	**339**	**303**	[4]
Tetra -CTS	**352**	**350**	**[4]**

Table: 3 summary of the Raman peaks location of CZTS phases after annealing.

VI. CONCLUSION

The purpose of presented work was to fabricate and analyze the thin film material Cu2ZnSnS4 (CZTS).the XRD measurement showed that the particle size was in micron range (~ 1.2 μm).the XRD graph confirmed tetragonal structure with lattice parameter, a=b=5.427 **Å**, c=10.84 **Å,** which is consistent with standard JCPDS, Data file - 260575.

The Raman shift of CZTS thin films shows that our samples are composed mainly by the CZTS phase, and confirmed that kesterite structure.

Fern leaf like shaped and flakes of CZT materials of morphology observed in 1to 500 nm scales of field emissions of scanning electron micrograph on the SS materials at room temperature deposited by electroplating at constant pH.

Tetragonal and diamond structure of CZTS materials observed at 800^0C on SS material.

XRD, RAMAN and FE-SEM result are consistent with CZTS phase materials.

VII. FUTURE SCOPE

Electro deposition for solar cells is an active area of research and it has been shown to provide improved benefits in several solar technologies. For the silicon solar cell contacts, electrodeposited metal contact result in 1-2 % solar cell efficiency improvement due to a lower processing temperature with better yield than screen printing, improved contact resistance, lower overall resistance, and the ability to fabricate small contacts that reflect the sunlight less.

For the chalcopyrite and the kesterite thin films, electro deposition offers very low cost of manufacturing with a continuous reel to reel or roll to roll process. Rigid glass or flexible metallic substrates can be used with these thin films. Potentially opening up new applications for solar energy, these applications span from energy generation for energy utilities to building integrated materials, solar- powered cars, and electronic devices. Electrodeposited CIGS is already scaled-up for manufacturing by solo power inc. for these applications, we expect that electro depositon will become a game changer in its ability to lower manufacturing costs to less than $ 0.50/ W, making solar energy affordable to public.

Unlike CIGS and CdTe, which have issues of materials availability such as indium, gallium, and tellurium and that are high cost, CZTS does not have these issues. Electrodeposited kesterite has the potential of reaching terawatt scale with the widest deployment in the marketplace.

REFERENCES

[1]. H.Katagiri, thin solid films 480/481, 426-432 (2005).
[2]. B, Ndiaye, C.Mbow, M.S. Mane and C. Sene, "One-step electrodeposited CUinSe2 absorber layer for efficient PV cells". Vol. 15 $N^0$4 (2012)609-620.
[3]. Minsung Jeon, Tomohiro Shimizu, Shoso Shingubara, Material letters 65(2011) 2364-2367.
[4]. P.A. Fernandes, P. M.P. Salome, A.F. da Cunha " Study of polycrystalline CZTS film by Raman scattering" (2011).
[5]. H. Katagiri, K. Jimbo, S. Yamada, T. Kamimura, W.S. Maw, T. Fukano, T. Ito, and T. MOtophiro, Appl.physics. Express 1, 041201 (2008).
[6]. Wang CE, Tanaka S, Shimizu T and Shingubara, "Journal of material Science nad Nanotechnology" volume 1/ Issue 1. ISSN 2348-9812.
[7]. Hariklia (Lili) Deligianni, Shafaat Ahmed, and Lubamyr T. Romankiw, "The Electrochemical Society Interace" – Summer 2011.
[8]. http://www.nillenium–project.org/
[9]. http://www.iea.org/

IJARSCT
ISSN (Online) 2581-9429
International Journal of Advanced Research in Science, Communication and Technology (IJARSCT)
International Open-Access, Double-Blind, Peer-Reviewed, Refereed, Multidisciplinary Online Journal
Impact Factor: 7.53
Volume 4, Issue 4, March 2024

[10]. en.wikipedia.org/wiki/semiconductor
[11]. en.wikipedia.org/wiki/Thin_film_solar_cell
[12]. en.wikipedia.org/wiki/Thin_film
[13]. http://coursenotes.mcmaster.ca/L04/Thin _films/Electrodeposition_of_Metal.pdf
[14]. Nanotechnology Science and practice: Sulbha K. Kulkarni.